

# An X-Band Quasi-Circulator GaAs MMIC

Laila Marzall, Zoya Popović

Department of Electrical Engineering, University of Colorado, Boulder  
Boulder, CO 80309, U.S.A.

laila.marzall@colorado.edu, zoya@colorado.edu

**Abstract**—This paper presents the design of a 8-12 GHz quasi-circulator fabricated in a 0.25  $\mu\text{m}$  GaAs pHEMT monolithic microwave integrated circuit (MMIC) process. The circuit consists of three Lange couplers which connect gates and drains of three equal gain-matched amplifiers. The coupling factor of the unequal-split Lange coupler is designed to achieve an isolation higher than 20 dB over a 40% bandwidth, with a return loss of better than 10 dB and an insertion gain of 2.4 dB across the band. The layout includes bias networks for the three amplifiers and occupies a 2.5 mm  $\times$  2.5 mm die. The compact quasi-circulator is intended for use in full-duplex front ends.

**Index Terms**—Active circulators; Quasi-circulators; Lange couplers; MMIC; MMIC circulators.

## I. INTRODUCTION

Circulators are used to enable full-duplex operation in microwave front-ends. Conventional ferrite circulators are passive components, but require the use of bulky permanent magnets for biasing, and are therefore not amenable to monolithic integration. Non-reciprocal behavior of transistors can be used to achieve circulation and was first presented in 1965 [1]. In these devices, the distinction is made between active 3-way circulators with full rotational symmetry as in a ferrite device, and quasi-circulators that have isolation between two of the ports but do not have full circulation. Different topologies of active MMIC circulators and quasi-circulators were demonstrated, e.g. in CMOS [2], [3] and GaAs [4], [5], [6].

Through-element circulators, concepts that use divider networks, as well as quasi-circulators based on passive isolation and phase cancellation, are presented in [7]. The use of quadrature hybrids is explored in [8], [9], [10]. Noise performance and power limitation analysis, as well as design techniques for simultaneous optimization are described in [11], [12], [13], [7] and [14]. Finally, integration with antennas is discussed in [15], [16], [17].

This work presents the design of a stable MMIC circulator with gain, using QORVO 0.25  $\mu\text{m}$  GaAs PHEMT devices and operating over X band (8-12 GHz). Small-signal amplifiers are used as non-reciprocal elements and phase cancellation is achieved with asymmetric Lange-couplers. Simulations are performed using NI AWR Microwave Office and the process design kit (PDK). Section II presents the circuit topology. Section III describes the design and MMIC layout main circuit components: the gain-matched unit amplifier used in each circulator branch, and the asymmetric Lange couplers.

This work was funded in part by CAPES - Coordenacao Aperfeicoamento de Ensino Superior (Brazil), and in part by Qorvo, Richardson, Texas, U.S.A..

Section IV presents the final circulator design and simulated performance. In conclusion, a comparison with previous works is summarized.

## II. ACTIVE CIRCULATOR TOPOLOGY AND DESIGN

A 6-port active circulator was first described in [18] and a MMIC design operating in the 0.2-2 GHz band reported in [4]. The topology is shown in Fig.1. Circulation is accomplished by connecting three unconditionally stable, gain-matched, single-stage equal amplifiers with three initially symmetric and equal Lange couplers. The *through* ports are connected to the amplifier inputs, and the *coupled* ports to the outputs. The isolated ports are terminated in 50- $\Omega$  resistors and the Lange coupling coefficient modified to achieve a trade-off between backward isolation ( $|S_{31}|$ ) and forward gain ( $|S_{21}|$ ), while ensuring stability. The forward gain of the circulator is proportional to the amplifier gain, reduced by the coupling and *through* attenuation of the Lange couplers.

The Lange couplers and unit amplifiers are first designed as independent sub-circuits and the layout is simulated using full-wave electromagnetic (EM) analysis using AWR-AXIEM. The layouts are then arranged in the final device and connected with 50- $\Omega$  lines. Several layout iterations are performed to ensure fit into an allocated 2.5 mm  $\times$  2.5 mm area, which includes the dicing (saw) streets.

## III. SUB-CIRCUIT DESIGN

This section presents the design of the unit amplifier and asymmetric Lange couplers, with EM-simulated performance and layouts.

### A. Unit Amplifier

Figure 2 shows the *IV* curves for a 6  $\times$  50  $\mu\text{m}$  fingers depletion-mode device. To achieve linearity and high gain, the device operates in class-A bias, leading to a gate and drain voltages of  $V_G = -0.4$  V and  $V_D = 5.4$  V.

The metal layer in this MMIC process supports a maximum current of 18 mA/ $\mu\text{m}$ , and the DC drain current at quiescent point is 39.5 mA. Line widths greater than 4  $\mu\text{m}$  are used to meet the current handling requirement of 72 mA with a safety margin. The biasing circuits are implemented with 3.95 nH spiral inductor RF chokes, 4 pF bypass and 0.9 pF blocking capacitors. To improve stability and increase bandwidth, a  $R = 200$   $\Omega$  feedback resistor is connected with high-impedance short lines between gate and drain terminals. The layout shown

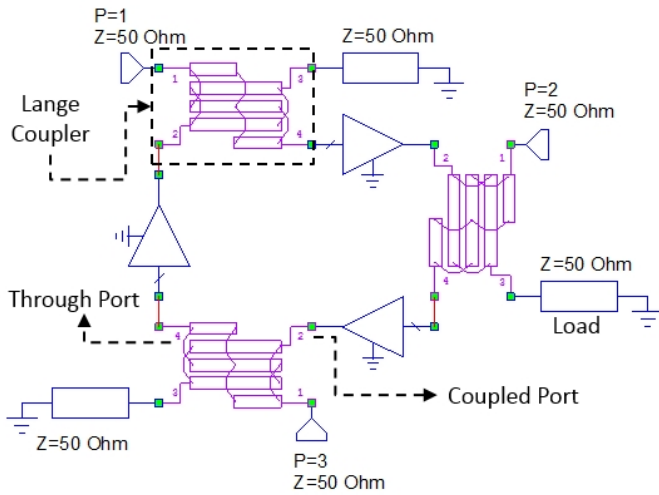


Fig. 1. Active circulator MMIC circuit topology. Nonreciprocal circulation is accomplished with gain-matched single-stage amplifiers. Each amplifier input is connected to a *through* port of one coupler while the output is connected to the *coupled* port of the following asymmetric Lange coupler. When port 1 (P1) is the input, P2 is the output and P3 isolated.

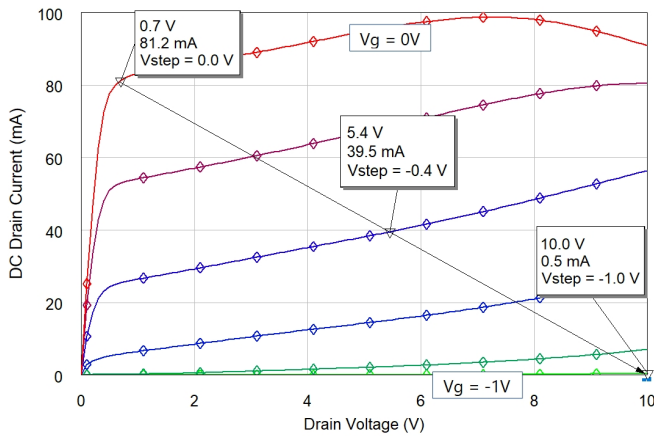


Fig. 2. Simulated *IV* curves for a 6-finger depletion-mode pHEMT showing the class-A operating point chosen for the design.  $V_G = -0.4$  V and  $V_D = 5.4$  V

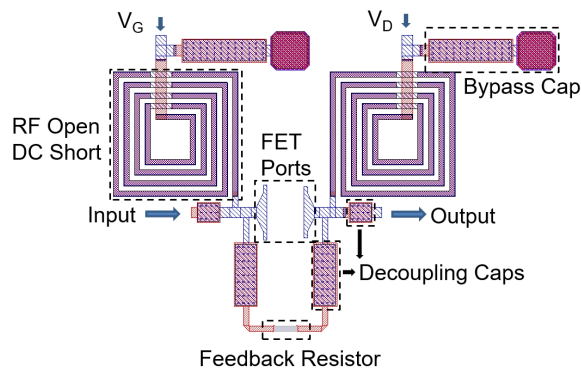


Fig. 3. Gate and drain bias circuit layout with a feedback resistor of  $200\ \Omega$  between the device gate and drain. Decoupling capacitors of  $0.9$  pF and bypass capacitors of  $4$  pF are used, with an RF choke implemented as a spiral inductor of  $3.9$  pF.

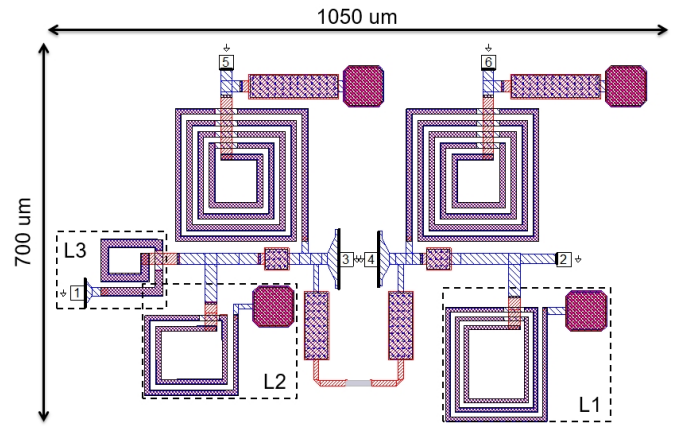


Fig. 4. Unit amplifier layout with a footprint of  $700\ \mu\text{m} \times 1050\ \mu\text{m}$ . The bias lines, transistor and feedback resistor determine the matching impedances at input and output. The matching circuits are designed with short transmission lines, two shunt inductors  $L_1$  and  $L_2$  and a series inductor  $L_3$ .

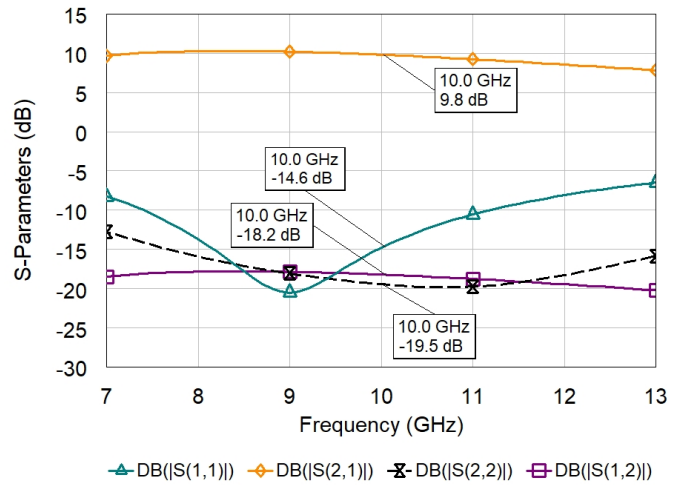


Fig. 5. EM-simulated unit amplifier *S*-parameters from 7 – 13 GHz.

in Fig.3 is fully EM-simulated and used to define gain-matched input and output reflection coefficients.

To design the gate and drain-side matching circuits, ideal tuners are connected to the input and output RF ports shown in Fig. 3. The output tuner is first swept to achieve a good match. This value is then fixed and the input tuner swept. After fine tuning, an input match  $\Gamma_{IN} = 0.57 \angle 116^\circ$  and  $\Gamma_{OUT} = 0.137 \angle 94^\circ$  are obtained. Matching networks are then designed with lumped elements because of size constraints.

Figure 4 shows the unit amplifier layout. Maximum dimensions are  $1050\ \mu\text{m} \times 700\ \mu\text{m}$ . Input and output matching networks are implemented with shunt inductors  $L_1 = 2.1$  nH and  $L_2 = 0.89$  nH, and a series inductor  $L_3 = 0.45$  nH. The EM-simulated *S*-parameters are plotted in Fig. 5, showing  $|S_{11}|$  and  $|S_{22}|$  below  $-10$  dB,  $|S_{21}| > 8$  dB and  $|S_{12}| < -15$  dB over  $8 - 12$  GHz.

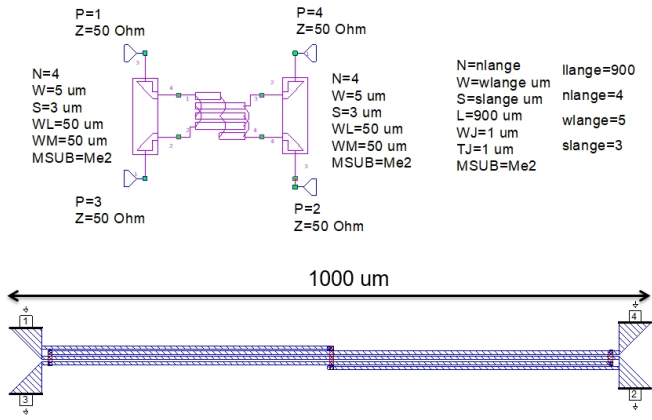


Fig. 6. Lange coupler simulation model (top), and geometry (bottom). The main geometric parameters are the number of lines ( $N = 4$ ), line widths  $w = 5 \mu\text{m}$ , line lengths  $L = 900 \mu\text{m}$ , and distance between lines  $s = 3 \mu\text{m}$ .

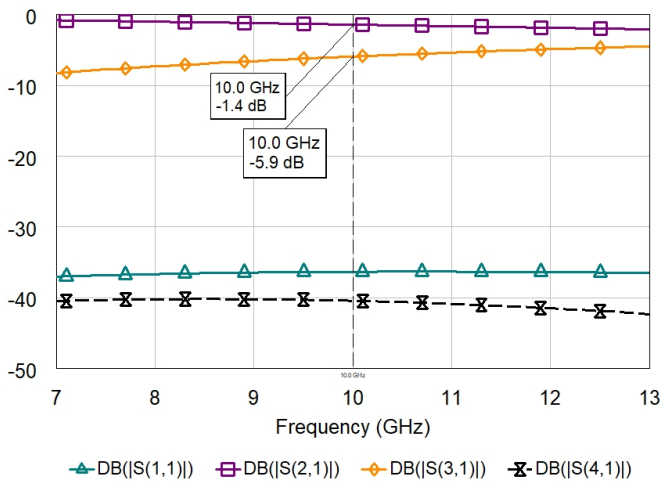


Fig. 7. Lange coupler EM-simulated  $S$ -parameters from 7–13 GHz.

### B. Asymmetric Lange coupler

The Lange coupler parameters are determined by adjusting the coupling coefficient to achieve the best circulator overall performance. The schematic and layout are shown in Figure 6. The EM-simulated results are plotted in Fig. 7 from 7–13 GHz showing an asymmetric power division with a relative high *through* of -1.4 dB to the direct port (P2) and a *coupled* level of -5.9 dB to P3. Match and isolation ( $|S_{11}|$  and  $|S_{41}|$ ) are below -30 dB over the band. The main geometric parameters are the number of lines ( $N = 4$ ), line widths  $w = 5 \mu\text{m}$ , line lengths  $L = 900 \mu\text{m}$ , and distance between lines  $s = 3 \mu\text{m}$ .

## IV. CIRCULATOR LAYOUT AND SIMULATED RESULTS

The final circulator geometry is displayed in Fig. 8. The RF GSG pads are connected by  $50 \Omega$  lines. The layout is adjusted to keep amplifier input and output lines the same length. Amplifier port geometries are individually remodeled so the layout fits in a  $2.5 \times 2.5 \text{ mm}^2$  area.

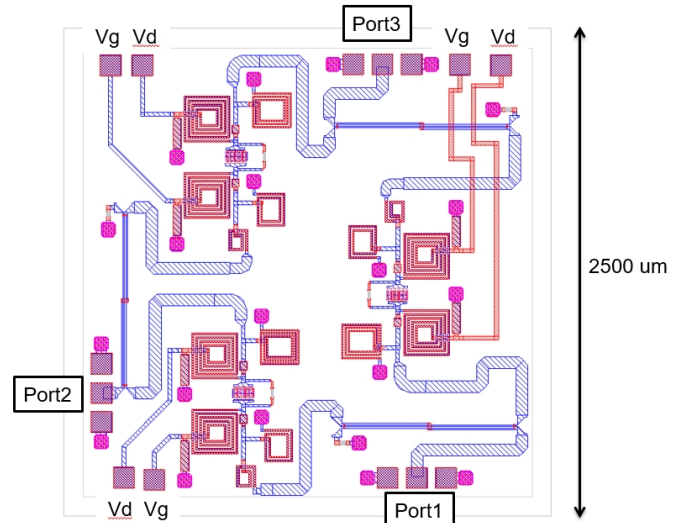


Fig. 8. Active circulator layout with perpendicular RF pads for ease of probing/packaging, and three sets of drain/gate bias pads.

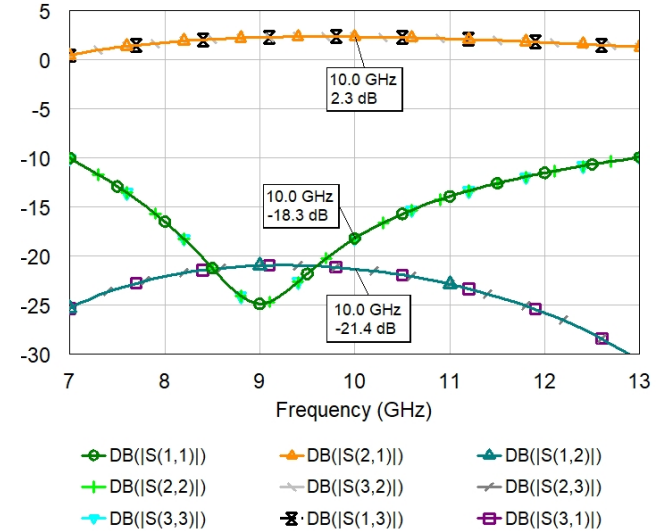


Fig. 9. Simulated active circulator  $S$ -parameters from 7 to 13 GHz showing insertion gain with isolation  $|S_{31}|$  greater than 20 dB.

The EM-simulation responses of each sub-circuit are placed in a schematic environment with transmission line models synthesizing interconnections and the circulator overall performance is simulated. The results are shown in Fig. 9. A gain of 2.4 dB at 10 GHz is observed between each pair of ports, with a return loss (RL) better than 14 dB and isolation (IS) better than 20 dB from 8–12 GHz, or an operating bandwidth of 40%.

In this circulator configuration, stability is a factor that needs to be carefully verified. The final design was EM-simulated over a wide frequency range and the stability factors  $K$  and  $B1$  (determinant) analyzed from DC to 20 GHz and is shown in Figure 10. Both parameters meet the unconditional stability condition ( $K > 1$ ,  $B1 > 0$ ) over the wide band for small-signal

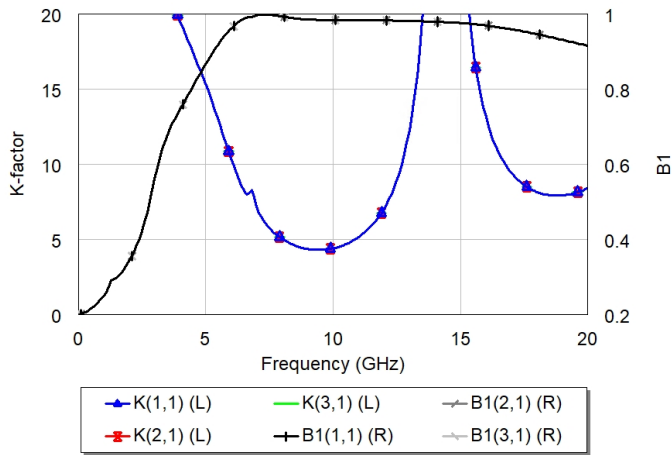


Fig. 10. Stability analysis for complete active circulator under nominal bias.

TABLE I  
COMPARISON OF ACTIVE MMIC CIRCULATOR PERFORMANCE [10]

Ref	BW (GHz)	$ S_{31} $ (dB)	$ S_{21} $ (dB)	$ S_{11} $ (dB)	Technology	Size (mm <sup>2</sup> )
This work	8 - 12	-20	2.5	-14	0.25 $\mu$ m GaAs pHEMT	6.25
[9]	10.2 - 12.6	-30	+1.5	<-17	0.25 $\mu$ m pHEMT	25
[19]	1.5 - 2.7	-26	+2	-10	CMOS	0.25
[2]	1.5 - 9.6	-18	-6	<-10	0.18 $\mu$ m CMOS	0.72 x 0.57
[13]	3.8 - 4.2	-22	+7.6	-15	MESFET	5
[20]	35 - 40	-30	-5	-15	0.25 $\mu$ m InP-HFET	1.75 x 1.9
[21]	6 - 18	-12	-2	-12	0.5 $\mu$ m GaAs MESFET	2.48 x 1.25
[6]	0.1 - 10	-16	7	-13	0.5 $\mu$ m GaAs FET	1.5 x 0.6

operation.

## V. CONCLUSION

The design of a stable active circulator MMIC with gain is presented. The device consists of three GaAs pHEMT amplifiers connected with asymmetric Lange couplers. A gain-matched amplifier design with resistive feedback results in a circulator with 2.4 dB forward gain, over 20 dB isolation and better than 14 dB from 8 to 12 GHz. Table I compares obtained results with previously published active circulators. Ongoing work includes investigation of different coupling levels, increased gain, large-signal behavior, power handling and increased isolation. Measurements on the fabricated GaAs MMIC are in progress.

## REFERENCES

[1] S. Tanaka, N. Shimomura, and K. Ohtake, "Active circulators amp;—the realization of circulators using transistors," *Proceedings of the IEEE*, vol. 53, no. 3, pp. 260–267, Mar. 1965.

[2] S. Shin, J. Huang, K. Lin, and H. Wang, "A 1.59.6 ghz monolithic active quasi-circulator in 0.18um cmos technology," *IEEE Microwave and Wireless Components Letters*, vol. 18, no. 12, pp. 797–799, 2008.

[3] K. Fang and J. F. Buckwalter, "A tunable 57 ghz distributed active quasi-circulator with 18-dbm output power in cmos soi," *IEEE Microwave and Wireless Components Letters*, vol. 27, no. 11, pp. 998–1000, 2017.

[4] I. J. Bahl, "The design of a 6-port active circulator," in 1988., *IEEE MTT-S International Microwave Symposium Digest*, 1988, pp. 1011–1014 vol.2.

[5] Y. Ayasli, "Field effect transistor circulators," in 1989 *IEEE International Magnetics Conference (INTERMAG)*, 1989, pp. AC2–AC2.

[6] S. Hara, T. Tokumitsu, and M. Aikawa, "Novel unilateral circuits for mmic circulators," *IEEE Transactions on Microwave Theory and Techniques*, vol. 38, no. 10, pp. 1399–1406, 1990.

[7] G. Carchon, B. Nauwelaers, S. Vandenberghe, and D. Schreurs, "Simultaneous power and noise optimization of active circulators," in 1998 *28th European Microwave Conference*, vol. 1, 1998, pp. 385–390.

[8] S. M. Hanna and J. Keane, "Analysis and applications of quadrature hybrids as rf circulators," in *Proceedings of International Conference on Particle Accelerators*, 1993, pp. 1118–1120 vol.2.

[9] S. Cheung, T. Halloran, W. Weedon, and C. Caldwell, "Active quasi-circulators using quadrature hybrids for simultaneous transmit and receive," in 2009 *IEEE MTT-S International Microwave Symposium Digest*, 2009, pp. 381–384.

[10] S. K. Cheung, T. P. Halloran, W. H. Weedon, and C. P. Caldwell, "Mmic-based quadrature hybrid quasi-circulators for simultaneous transmit and receive," *IEEE Transactions on Microwave Theory and Techniques*, vol. 58, no. 3, pp. 489–497, 2010.

[11] S. Furukawa and S. Horiguchi, "The noise performance of the active circulator," *Proceedings of the IEEE*, vol. 55, no. 11, pp. 2048–2050, Nov. 1967.

[12] A. Gasmi, B. Huyart, E. Bergeault, and L. Jallet, "MMIC quasi-circulator with low noise and medium power," in *Proc. IEEE MTT-S Int. Microwave Symp. Digest*, vol. 3, Jun. 1996, pp. 1233–1236 vol.3.

[13] A. Gasmi, B. Huyart, E. Bergeault, and L. Jallet, "Noise and power optimization of a mmic quasi-circulator," *IEEE transactions on microwave theory and techniques*, vol. 45, no. 9, pp. 1572–1577, 1997.

[14] G. Carchon and B. Nanwelaers, "Power and noise limitations of active circulators," *IEEE Transactions on Microwave Theory and Techniques*, vol. 48, no. 2, pp. 316–319, Feb. 2000.

[15] M. J. Cryan, P. S. Hall, K. S. H. Tsang, and J. Sha, "Integrated active antennas with simultaneous transmit-receive operation," in *Proc. 26th European Microwave Conf.*, vol. 2, Sep. 1996, pp. 565–568.

[16] M. J. Cryan and P. S. Hall, "An integrated active circulator antenna," *IEEE Microwave and Guided Wave Letters*, vol. 7, no. 7, pp. 190–191, Jul. 1997.

[17] A. Ohlsson, V. Gonzalez-Posadas, and D. Segovia-Vargas, "Active integrated circulating antenna based on non-reciprocal active phase shifters," in *Proc. Second European Conf. Antennas and Propagation EuCAP 2007*, Nov. 2007, pp. 1–5.

[18] M. A. Smith, "Gaas monolithic implementation of active circulators," in 1988., *IEEE MTT-S International Microwave Symposium Digest*, 1988, pp. 1015–1016 vol.2.

[19] Y. Zheng and C. E. Saavedra, "Active quasi-circulator mmic using otas," *IEEE Microwave and Wireless Components Letters*, vol. 19, no. 4, pp. 218–220, 2009.

[20] M. Berg, T. Hackbarth, B. Maile, S. Koslowski, J. Dickmann, D. Kother, B. Hopf, and H. Hartnagel, "Active circulator mmic in cpw technology using quarter micron inalas/ingaas/inp hfets," in *Proceedings of 8th International Conference on Indium Phosphide and Related Materials*. IEEE, 1996, pp. 68–71.

[21] P. Katzin, Y. Ayasli, L. D. Reynolds Jr, and B. E. Bedard, "6 to 18 ghz mmic circulators," vol. 35, 01 1992.